行政院國家科學委員會專題研究計畫　成果報告

調制結構的電場及磁場效應的 X-光散射實驗

計畫類別： 個別型計畫
計畫編號： NSC92-2112-M-032-013-
執行期間： 92 年 08 月 01 日至 93 年 07 月 31 日
執行單位： 淡江大學物理系

計畫主持人： 杜昭宏

報告類型： 精簡報告

處理方式： 本計畫可公開查詢

中　華　民　國 93 年 12 月 6 日

一 緣由與目的

Since the discovery of high-T_C superconductors and materials possessing the properties of colossal magnetoresistance (CMR), the coupling interactions between the degree of freedoms of electron, spin, orbital, and lattice have been a subject of extensive investigation in solid state physics. Among these transition metal oxides, the modulations due to the formations of charge, orbital and spin ordering are the common characteristic, and accompanying with the occurrence of the unusual transport behaviour. For instance, the incommensurate modulations due to the formation of dynamic charge and spin stripes have been only observed in the hole-doped cuprates ($La_{2-x}Sr_xCuO_4$) showing superconducting state at low temperatures, and the incommensurability of the modulations is determined by the concentrations of the holes. The colossal magnetoresistance as that observed in manganits has also been demonstrated to be strongly correlated to the formation of the charge, orbital, and spin stripes. In addition, these modulations (charge, orbital and spin stripes) coupling to the lattice produce a very rich phase diagram. Experimentally, these modulated structures have been extensively studied using x-ray and neutron scattering and electron diffraction techniques and have been theoretically demonstrated to play an important role on the transport behaviour. Nevertheless, the detailed and direct probes of the correlations between the modulations and the applied fields (either electric or magnetic) are still of lack. In order to clarify the role played by the modulations in the strongly correlated electrons system, we attempt to investigate the responses of the modulations to the applied fields (electric and magnetic fields) in two high-T_C superconductor related compounds $La_{2-x}Sr_xNiO_4$ and $ARuO_3$ (A=Sr, Ba, Ir) using x-ray scattering.

二 英文摘要

In order to get the experience on the field effects of modulated structure, we started with the measurements on the conventional quasi-one dimensional material $K_{0.3}MoO_3$ because its transport behaviour has been widely studied. In this experiment, by means of multiple x-ray diffraction, we demonstrated that the nonlinear conductivity is through the internal distortion of the CDW (charge-density waves) lattice as the applied voltages approaching to the threshold value. In addition, we also demonstrate that the CDW lattice can be drove to move through the dynamic phase transition, i.e., from the pinning state to a moving solid state, and finally to a disordered moving liquid, as the applied fields exceeding the threshold value.

Keywords: charge-density waves (CDWs), multiple x-ray diffraction, x-ray scattering, creeping phase, plastic flow, moving solid

三 結果與討論

The dynamic behaviour of the periodic media with lattice imperfections is ubiquitous and long-standing problem in many condensed material systems, because of the correlation to the unusual physical phenomena, for instance, the charge-density waves/spin-density waves to the

nonlinear conductivity, the charge/spin stripes to the CMR and the high-T_C superconductivity[1], and the vortex lattice to superconductivity[2]. In static systems, the imperfections in a medium result in a disordered ground state which prevents the system from forming a long-range order at low temperatures, therefore giving rise to unusual physical properties. In dynamic systems under a driving force, the disordered medium produces a more fascinating phase diagram[3,4]. Analogous to the vortex lattice, the inhomogeneous distribution of charge densities also forms a periodic lattice below the transition temperature, namely charge-density waves (CDWs). Combining x-ray scattering and multiple diffraction, we demonstrate that the CDW lattice can be driven by a driving force to move and undergo a dynamic phase transition, i.e. from the disordered pinning state → ordered moving solid state → disordered moving liquid, and the nonlinear conductivity occurs through a phase jump of 2π.

Nonlinearity is commonly observed in a very broad range of natural phenomena, from classical/quantum mechanics to biology, such as the squeezed states in a Bose-Einstein condensation[5] and the conduction of DNA[6]. The character of such behaviour is the changes of the symmetry or the length-scale of the states in the system. In condensed materials, the nonlinear physical properties always go along with the formation of a periodically modulated lattice caused by the inhomogeneous distribution of charges or spins, namely charge or spin density waves, for instance, the nonlinear conductivity observed in $K_{0.3}MoO_3$, and 2*H*-$NbSe_2$, or charge/spin stripes [1, 7] in high-T_C superconductors and $La_{2-x}Sr_xNiO_4$, or other strongly correlated electron systems. In a system involving the instability of charge densities, its ground state can be expressed as $\rho = \rho_o\left[1+\sum_i P_i\cos(2\pi Q_i\cdot r+\varphi_i)\right]$ where the ρ_0 is the undistorted electron density, P_i the distorted amplitude, $\vec{Q}_i$ the wavevector of the modulation, and φ_i the phase[8]. The appearance of imperfections distorts the lattice, and the phases φ_i are pinned by the imperfections. It has been demonstrated that the phase φ_i governs the dynamic behaviour of this modulated lattice and is therefore responsible for the occurrence of the unusual physical phenomena**,** such as the pinning and memory effects and sliding behaviour[9]. In this Latter, we demonstrate that the CDW lattice undergoes a dynamic phase transition as the applied voltage exceeding the threshold. We also experimentally demonstrate that the occurrence of nonlinear conductivity is through an internal deformation of the lattice which results in a 2π phase jump[10].

A good quality single crystal $K_{0.3}MoO_3$ being a quasi-one dimensional material was used for this study. The crystal structure belongs to the monoclinic system with a space group *C2/m*. The lattice parameters[11] of $K_{0.3}MoO_3$ are a =18.162 Å, b = 7.554 Å, c = 9.816 Å, and β = 117.393°. The sample was characterized to have a mosaic width of ~0.005° and pre-aligned using an x-ray rotating anode source. The *in-situ* measurements were carried out on the beamline BL12B2 of SPring-8 synchrotron facility. Two gold stripes spaced ~3 mm were evaporated onto the sample surface as shown in the inset of Fig. 1, so that the voltage was applied along the b^*, [010], axis. The sample was glued on the cold head of a cryostat mounted on a 6-circle diffractometer. A Keithely 2400 source meter was used to generate the driving voltage, and the *I-V* curve was measured in the two-probe setup.

Figure 1 shows the non-linear conductivity of the sample at T=70 K, indicating the transition from pinned CDWs to sliding CDWs. Best fits to the data for the low voltage region, the *I-V* curve can be fitted well by an exponential formula as reported by Ogawa et al. [13], indicating a CDW creeping behaviour. However, we did not observe the hysteretic switching phenomenon[14] at V_C for T=70 K because of thermal fluctuations smearing out the switching transition[15]. The threshold for the sliding CDWs extracted from the fits to a power law, $I \propto (\frac{V - V_C}{V_C})^{\beta}$, gives to V_C = 0.165 V and the exponent β = 1.114, suggesting that the sliding CDWs are a dynamic critical behaviour[16~19]. The threshold voltage V_C for sliding CDWs was also confirmed by a plot of *d*R/*d*V versus V (the inset of Fig.1).

The evolution of CDW satellite reflection as a function of voltage was probed *in-situ* using x-ray scattering. Since the formation of density modulations occurs at $Tc \approx 180$ K, the sample was cooled down to 70 K. The satellite reflection was located at the Bragg position G = (13 q 6.5), where q ~ 0.748. Scans were performed through the longitudinal direction of [2 0 -1], and the data were convoluted with the x-ray resolution function obtained from the nearby Bragg peak (12

0 -6). In Fig. 2a, below $V_C \sim 0.165$ V, where the creeping CDWs occur, the FWHM widths remain unchanged. This means that the ordering of the quenched disordered CDWs was not altered by the low driving force in this region. Beyond the threshold V_C, the CDW reflection is getting sharper but weaker. This can be understood that a driving force steers a pinned lattice and results in inhomogeneous flow[20, 21]. As the driving force exceeding the threshold, $V_C \sim 0.165$ V, the CDW lattice reorders along the longitudinal direction [2 0 -1] transverse to the field direction. As the CDWs are driven to sliding along the [0 1 0], the coupling between the chains is further reduced[22], and then could result in the transition toward the smectic type of order[3, 23] in the region II. In this region, because of lacking switching behaviour at the threshold V_C, the moving of CDW lattice can be described as the critical phenomenon of a classical field associated with distortions, and is still in an elastic flow state[14, 18]. As the voltage exceeding 0.18 V, the lattice shows a long-rang ordered state; temporal order. This motional ordered behaviour by a driving force has also been reported [22] in the $NbSe_3$. In contrast to the lattice existing nearby the threshold ($V_C = 0.165$ V), where both pinned and flowing regions coexist, there only flowing part remains in this motional ordered state; namely a moving solid phase[12, 22, 19]. When V > 0.22 V, we observed continuous broadening of the width and decreasing in the amplitude of the diffraction peak as like the critical scattering, indicating that the moving solid phase started deforming, and then became a moving electronic liquid phase.

The other key quantity we studied in this Letter is the triplet phase δ_3 of a 3-wave multiple diffraction at different biased voltages. To set up a 3-wave (***O***,***G***,***L***) multiple diffraction experiment, the crystal is first aligned for a reflection *G*, the so-called primary reflection. It is then rotated around the reciprocal lattice vector ***G*** with an azimuthal angle ψ to bring in the secondary reflection *L* which also satisfies Bragg's law. Namely, both *G* and *L* reflections take place simultaneously. ***O*** stands for the incident reflection. The interaction of the multiply diffracted waves modifies the intensity of the primary reflection. Intensity variation showing asymmetric distribution versus ψ gives the information about δ_3, which is the phase of the structure-factor triplet $F_L F_{G-L}/F_G$, where F_G, F_L, and F_{G-L} are the structure factors of the primary reflection *G*, the secondary *L*, and the coupling reflection *G-L* involved in the 3-wave

diffraction[24~26]. Previously[27], we demonstrated that the triplet phase δ_3 due to the coupling between the CDW lattice and its host lattice can be probed using multiple diffraction. Here we further demonstrate that measuring the relative change in $\delta_3, \Delta\delta_3$, caused by a driving force, makes the study of the internal deformation of the CDW lattice possible.

We concentrated on the particular three-wave diffraction, (0 0 0), (13 *q* -6.5) and (4 -8 4) at ψ=108.53^o, where the primary reflection is (13 *q* -6.5) and the coupling reflection is (9 8+*q* 10.5). The profile asymmetry of the diffraction intensity of (13 *q* -6.5) versus ψ at *V*= 0 is typical for δ_3=0. The phase variation $\Delta\delta_3$ due to non-zero applied voltages was analyzed based on the dynamical theory for multiple diffractions[24~26]. In Fig. 3, the profile develops different asymmetry at different finite voltages. In the static CDW state, the crystal lattice possesses a centrosymmetric structure, and a change in the peak profile means that this centrosymmetry is broken due to the relative motion of ions by a driving force. This results in a non-zero of $\Delta\delta_3$. As shown in figure 2b, the $\Delta\delta_3$ reaches to the top at *V* = 0.12 ~ 0.14 V. This can be understood as the internal distortion of CDWs is saturated just before the sliding motion. Classically, upon the application of bias voltage, the free energy is minimized by the elastic energy cost due to CDW distortion. After threshold, it is energetically favourable to slid (increasing kinetic energy) rather holding up the large elastic energy. The estimated $\Delta\delta_3$ from curve fitting at 0.1, 0.12 0.13, 0.14, 0.15, and 0.16 V are about 6^o, 10^o, 18^o, 17^o, 17^o, and 10^o respectively, and then back to 0^o for V > 0.18 V, as shown in Figs. 4 and 2b. This evidences experimentally that the occurrence of non-linear transport behaviour is through a phase jump of 2π at the sliding threshold, i.e., from the pinned to sliding states.

Based on all experimental results given above, the simultaneous studies on *I-V* curve, the relative phase change $\Delta\delta_3$, and the ordering the CDWs as a function of driving voltage have provided evidence for the origin of the nonlinearity and the dynamic phase transition of a periodic medium. While it is already exciting to observe these dynamic motions of CDW, it also opens up many interesting issues requiring further studies. For instance, crossovers between

different types of dynamics could be achieved by varying temperatures, and a global phase diagram can be mapped out completely by varying temperature and driving force, and deepen our understanding of the dynamic motions of a periodic medium such as that existing in the high-T_C related perovskites.

四 計畫成果

This experiment can not be done without the grant support from NSC. The result has been written into two papers. One is titled as "X-ray Multiple-wave Interaction in a Quasi-two-dimensional Material 2H-$NbSe_2$", and has been published on Acta Crystallographic **A 60**, 209-213 (2004). The second one is "Nonlinearity and dynamic phase transition of the CDW lattice", which will be submitted to PRL.

References:

1. Littlewood, P., Phases of resistance, *Nature* **399**, 529-530 (1995)

2. Yaron, U. *et al.* Structural evidence for a two-step process in the depinning of the superconducting flux-line lattice, *Nature* **376**, 753-755 (1995).

3. Giamarchi, T. and Doussal, P. Le, Elastic theory of flux lattices in the presence of weak disorder, Phys. Rev. **B 52**, 1242-1270 (1995)

4. Balents, L., Marchetti, M. C. and Radzihovsky, L., Nonequilibrium steady states of driven periodic media, Phys. Rev. **B 57**, 7705-7739 (1998)

5. Rolston, C. L. & Phillips, W. D., Nonlinear and quantum atom optics, *Nature* **416**, 219-224 (2002)

6. Porath, D. *et al.* Direct measurement of electrical transport through DNA molecules, *Nature* **403**, 635-638 (2000)

7. Du, C.-H. *et al.* Critical Fluctuations and Quenched Disordered Two-Dimensional Charge Stripes in $La_{5/3}Sr_{1/3}NiO_4$, Phys. Rev. Lett. **84**, 3911-3914 (2000)

8. Overhauser, A. W., Charge-density waves and isotropic metals, Adv. Phys. **27**, 343 (1978)

9. Grüner, G., *Density waves in solids*, (Addison-Wesley, New York, 1994)

10. Brazovskii, S. *et al.* Plastic sliding of charge density waves: X-ray space resolved-studies versus theory of current conversion. Phys. Rev B. **61**, 10640-10650 (2000).

11. Schutte, W. J. and Bore, J. L. de, The incommensurately modulated structures of the blue bronzes $K_{0.3}MoO_3$ and $Rb_{0.3}MoO_3$, Acta Cryst. **B 49**, 579-591 (1993)

12. Lemay, S. G. *et al.* Temporally ordered collective creep and dynamic transition in the charge-density wave conductor $NbSe_3$, Phys. Rev. Lett. **83**, 2793-2796 (1999)

13. Ogawa, N. *et al.* Photocontrol of dynamic phase transition in the charge-density wave material $K_{0.3}MoO_3$, Phys. Rev. Lett. **87**, 256401 (2001)

14. Vinokur, V. M. and Nattermann, T., Hysteretic depinning of anisotropic charge density waves, Phys. Rev. Lett. **79**, 3471-3474 (1997)

15. Adelman, T. L. *et al.* Low-temperature charge-density-wave dynamics and switching in $NbSe_3$, Phys. Rev. **B 47**, 4033-4036 (1993)

16. Chauve, P., Giamarchi, T. and Doussal, P. Le, Creep and depinning in disordered media, Phys. Rev. **B 62**, 6241-6267 (2000)

17. Marchetti, M. C., Middleton, A. A., Saunders, K. and Schwarz, J. M., Driven depinning of strongly disordered media and anisotropic mean-field limits, Phys. Rev. Lett. **91**, 107002 (2003)

18. Fisher, D. S., Threshold behaviour of charge density waves pinned by impurities, Phys. Rev. Lett. **50**, 1486-1489 (1983)

19. Chen, L.-W. *et al.* Dynamic transition in sliding charge-density waves with quenched disorder, Phys. Rev. **B 54**, 12798-12806 (1996)

20. Koshelev, A. E. and Vinokur, V. M., Dynamic melting of the vortex lattice, Phys. Rev. Lett. **73**, 3580-3583 (1994)

21. Reichhardt, C. *et al.* Dynamical ordering of driven stripe in quenched disorder, Phys. Rev. Lett. **90,** 26401 (2003)

22. Danncau, R. *et al.* Motional ordering of a charge-density wave in the sliding state, Phys. Rev. Lett. **89**, 106404 (2002)

23. Doussal, P. Le. and Giamarchi, T., Moving glass theory of driven with disorder, Phys. Rev. **B 57**, 11356 (1998)

24. Chang, S.-L., *X-ray multiple-wave diffraction: theory and application* (Springer-Verlag, Berlin, 2004)

25. Colella, R., Multiple diffraction of X-rays and the phase problem. Computational procedures and comparison with experiment, Acta Crystallogr. **A 30**, 413-423 (1974);

26. Shen, Q., Solving the Phase Problem Using Reference-Beam X-Ray Diffraction, Phys. Rev. Lett. **80**, 3268-3271 (1998).

27. Du, C.-H. *et al.* X-ray multiple-wave coherent interaction in a quasi-two dimensional material 2*H*-$NbSe_2$, Acta Cryst. **A 60**, 209-213 (2004)

Acknowledgements:

We are gratefully to the National Science Council, Ministry of Education and the National Synchrotron Radiation Research Centre, Taiwan, for funding this research. The beam time arrangements by the NSRRC and SPring-8 are also gratefully acknowledged.

Figure legends:

Figure 1: *I-V* curve: The red line is the fit to an exponential formula which is due mainly to the thermally activated moving of CDW condensates. The green line is the fit to a power law, giving a sliding threshold V_C = 0.165 V and an exponent β = 1.114. The left inset shows the dimension of the sample and the experimental setup. The right inset, (dR/dV) shows a transition point at V_C = 0.165 V. An upper limit of the current was set to be 300 mA to protect the sample and meter.

Figure 2: Measurements vs. voltage: (**a**) The evolution of the peak width as a function of voltage. The changes of the curves can be divided into three regions; I the creeping CDW state, II the moving solid, and III the moving liquid. The widths are in the reciprocal lattice unit (r.l.u). (**b**) The evolution of the relative phase change $\Delta\delta_3$ as a function of voltage. The δ_3 changes only as the driving force approaching to the threshold, suggesting a phase jump of 2π from the pinned to the sliding CDWs.

Figure 3: Evolution of the 3-wave diffraction profile as a function of voltage: The profile develops different asymmetry only at voltages of 0.12, 0.13, and 0.14 V in accord with the regime for a creeping CDW state. This change results from the change of the triplet phase δ_3. At these voltages, the Darwin widths of the reflections remained the same. This makes sure that the crystal does not destroyed by applied voltages.

Figure 4: Curve-fitting of the 3-wave diffraction profiles for $\Delta\delta_3$ at V= 0.2 mV and 0.14 V: Since the primary (13 q -6.5) and the coupling reflection (9 8+q 10.5) are the fractional reflections, their structure factor amplitudes are much smaller than that of the secondary (4 -8 4) reflection. Also the amplitudes of (13 q -6.5) are nearly the same for V< 0.18 V. Under this condition, the modification of profile asymmetry is dominated by the phase, rather than the amplitude of the structure-factor triplet. The analysis is based on the dynamic theory for multiple diffraction, giving $\Delta\delta_3 = 0$ and 18^o at V= 0 and 0.14 V, respectively.

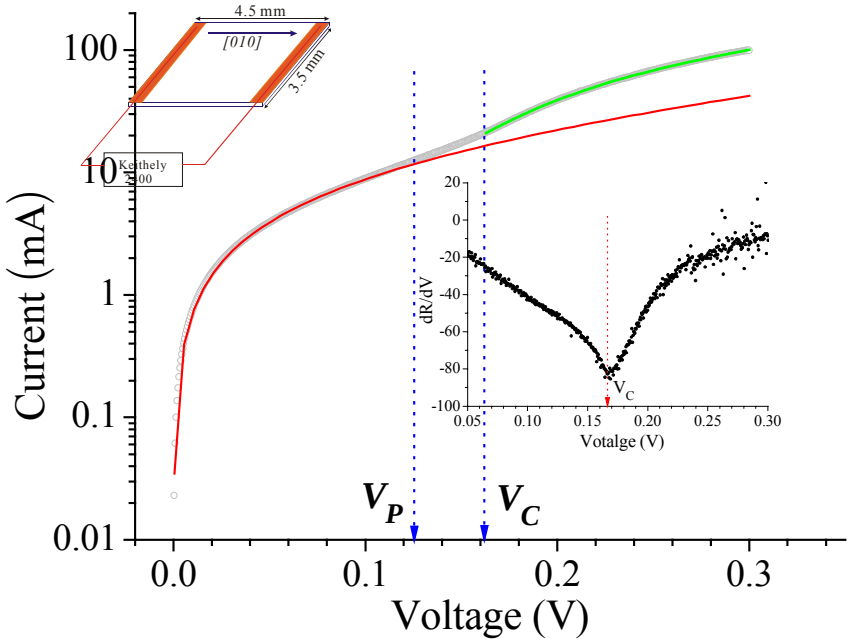

Figure 1

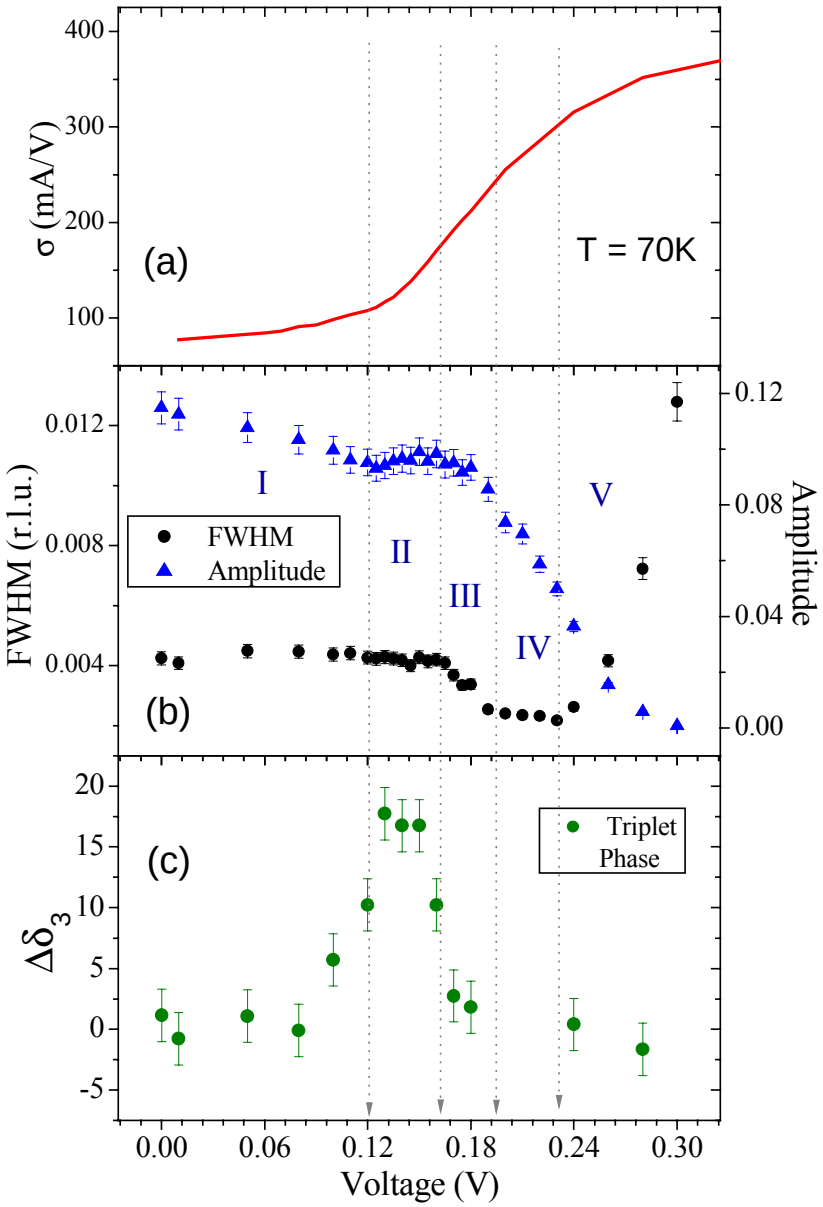
σ (mA/V)
400
300
200
100
(a)
T = 70K
FWHM (r.l.u.)
0.012
0.008
0.004
0.12
0.08
0.04
0.00
Amplitude
FWHM
Amplitude
I
II
III
IV
V
(b)
$\Delta\delta_3$
20
15
10
5
0
-5
(c)
Triplet
Phase
0.00
0.06
0.12
0.18
0.24
0.30
Voltage (V)

Figure 2

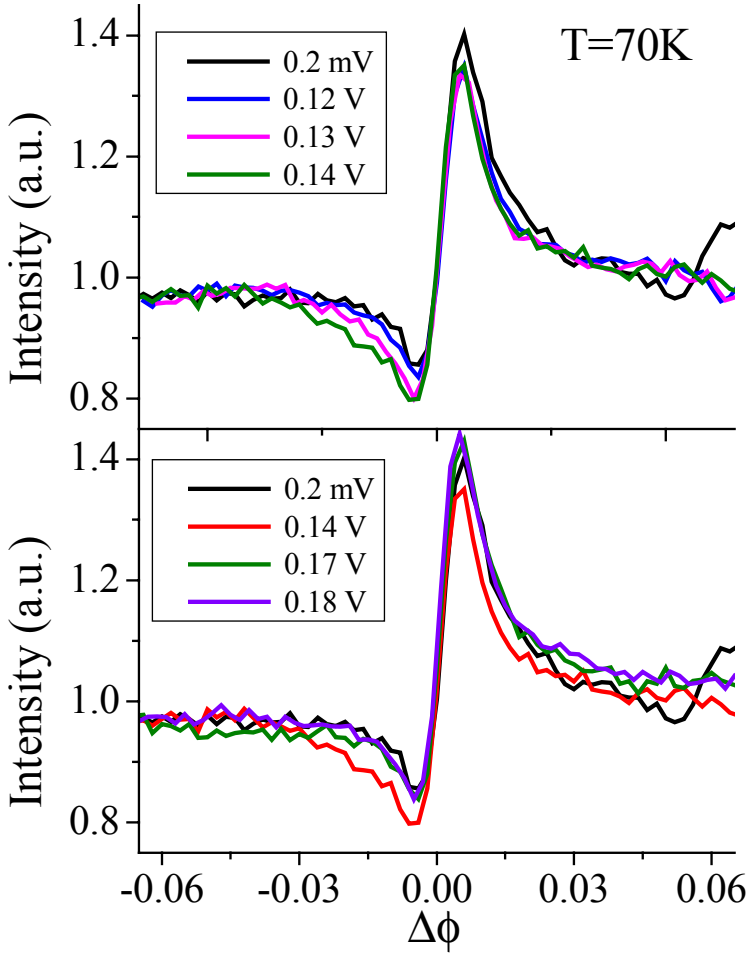
T=70K
0.2 mV
0.12 V
0.13 V
0.14 V
Intensity (a.u.)
1.4
1.2
1.0
0.8
0.2 mV
0.14 V
0.17 V
0.18 V
Intensity (a.u.)
1.4
1.2
1.0
0.8
-0.06
-0.03
0.00
0.03
0.06
Δϕ

Figure 3

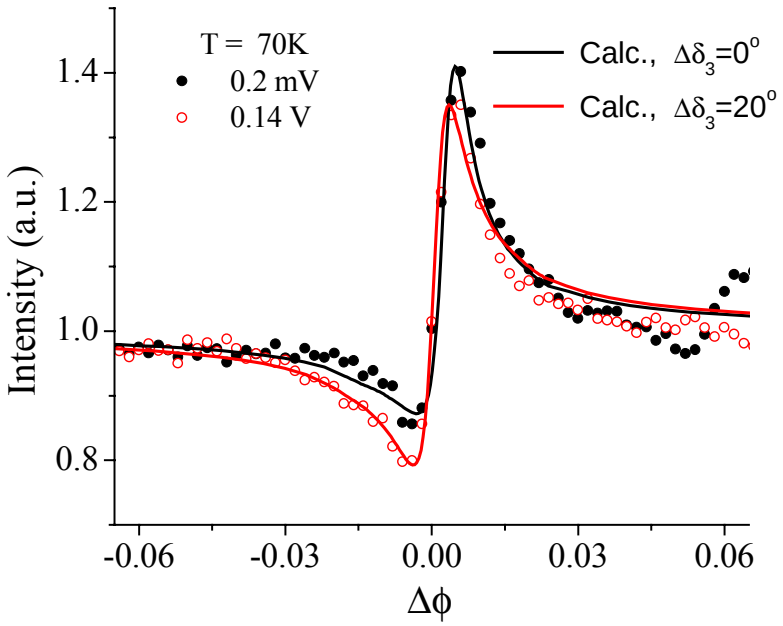
T = 70K
0.2 mV
0.14 V
Calc., Δδ3=0°
Calc., Δδ3=20°
Intensity (a.u.)
1.4
1.2
1.0
0.8
-0.06
-0.03
0.00
0.03
0.06
Δϕ

Figure 4